Advances in Difference Equations
a SpringerOpen Journal

RESEARCH Open Access

Modeling the health impact of water and sanitation service deficits on waterborne disease transmission

Rujira Chaysiri[1], Garrick E. Louis[2] and Wirawan Chinviriyasit[3*]

*Correspondence:
wirawon.chi@kmutt.ac.th
[3]Department of Mathematics, Faculty of Science, King Mongkut's University of Technology Thonburi, Bangkok, Thailand
Full list of author information is available at the end of the article

Abstract

Cholera is a waterborne disease that continues to pose serious public health problems in many developing countries. Increasing water and sanitation coverage is a goal for local authorities in these countries, as it can eliminate one of the root causes of cholera transmission. The SIWDR (susceptible–infected–water–dumpsite–recovered) model is proposed here to evaluate the effects of the improved coverage of water and sanitation services in a community at risk of a cholera outbreak. This paper provides a mathematical study of the dynamics of the water and sanitation (WatSan) deficits and their public health impact in a community. The theoretical analysis of the SIWDR model gave a certain threshold value (known as the basic reproductive number and denoted $\mathcal{R}_0$) to stop the transmission of cholera. It was found that the disease-free equilibrium was globally asymptotically stable whenever $\mathcal{R}_0 \leq 1$. The unique endemic equilibrium was globally asymptotically stable whenever $\mathcal{R}_0 > 1$. Sensitivity analysis was performed to determine the relative importance of model parameters to disease transmission and prevention. The numerical simulation results, using realistic parameter values in describing cholera transmission in Haiti, showed that improving the drinking water supply, wastewater and sewage treatment, and solid waste disposal services would be effective strategies for controlling the transmission pathways of this waterborne disease.

Keywords: Water and sanitation; Waterborne disease; Global stability; Lyapunov function; Cholera

1 Introduction

The most common waterborne diseases that pose a major public health risk in communities and continue to be leading causes for illnesses and deaths worldwide, especially in developing countries, include diarrhea, cholera, giardia, dysentery, Escherichia coli, salmonella, shigella, typhoid, and hepatitis A [1]. Waterborne diseases are caused by a lack of safe drinking water and proper sanitation, which is a major cause [2]. According to the World Health Organization (WHO), cholera is an infectious disease characterized by severe watery diarrhea and is caused by eating food or drinking water contaminated with the bacterium *Vibrio cholerae*. Diarrhea kills an estimated 829,000 people globally each year as a result of contaminated drinking water, sanitation, and hand hygiene [3]. In

addition, morbidity and mortality are worse in developing countries where communities lack the resources to provide sustained access to adequate water and sanitation services [4]. For instance, in 2010, Haiti suffered from a cholera outbreak with 665,000 cases and 8,183 deaths [5]. A cholera outbreak also occurred in Yemen in 2016 with more than 1.2 million cases and 2,500 deaths, of which 30% were children under the age of five [6]. In many low income countries, inadequate investment in water and sanitation infrastructure has perpetuated the problem. The inadequate investment resulted in illnesses among citizens. Loss of work productivity due to illnesses lowered individual income; hence, there was a lower national income. Consequently, low income countries had the least amount of money to invest in water and sanitation infrastructure that is necessary to combat the burden of waterborne diseases [7, 8]. Furthermore, open dumpsites in developing countries play an important role in the transmission of diseases [9, 10]. Open dumpsites can be an important and large reservoir of pathogens in these communities. Pathogens in open dumpsites can get into water sources through leachate, which contaminates unprotected groundwater sources, or through precipitation and runoff into surface water [11–13]. For example, open dumpsites in Yemen are located close to communities. This situation increases the health risks in these communities, especially from clinical waste, which has been demonstrated to contribute to cholera outbreaks in Yemen [14].

Since the connections between unclean water, sanitation, and health are well established [7, 15–17], combating waterborne diseases requires multiple strategies. These strategies include increasing access to safe drinking water and improved sanitation and cutting disease transmission pathways by having good hygiene practices [18]. According to the WHO, 94% of diarrhea cases are preventable by healthy environments, which include increasing access to clean water and sanitation services, and improved hygiene [19]. For sanitation services [7, 20], systematic reviews concluded that improved sanitation can reduce diarrhea cases by 32%–37%. This indicates that providing adequate safe drinking water and sanitation services reduces the incidence of acute infectious diarrhea [21–23]. Moreover, a study in Brazil and El Salvador found that improving sewerage coverage led to a significant reduction in diarrhea prevalence [24–27]. In this paper, therefore, the impact of improving water and sanitation services and the management of open dumpsites are explored as mechanisms to control waterborne disease transmission.

Mathematical models have been used to understand the transmission dynamics of waterborne disease, to improve control and prevention strategies, and to inform public health impacts [28–32]. Tien and Earn [28] presented the susceptible–infected–recovered (*SIR*) model with pathogen concentration, which was called the susceptible–infected–water–recovered (*SIWR*) model when applied to waterborne disease transmission. Their study showed that applying the *SIR* model rather than using the *SIWR* model underestimates the basic reproductive number and overestimates the infectious period when the pathogen decay rate is slow in the water compartment. Eisenberg *et al.* [29] showed that parameters in the *SIWR* model were globally identifiable. They estimated this by using the data from a cholera outbreak in Angola as a case study. Also, their study concluded that including environmental data was important when analyzing waterborne diseases. The *SIWR* model was further extended by having multiple patches within a common water resource. Their model assumed that the human-to-human transmission pathway occurs within a patch and the environment-to-human pathway happens across multiple patches with a shared water resource. Their study also explored the effects of heterogeneity on the final size of

an outbreak and the efficiency of interventions [30]. This type of spatially explicit model [31–33] was also used to investigate waterborne disease epidemics that account for local communities of susceptible and infected individuals in a spatially explicit arrangement of nodes linked by networks having different topologies. A network epidemic model of waterborne disease was studied by Wang and Cao [34] and Collins and Govinder [35]. These models considered the heterogeneity of different water sources that were contaminated. The optimal control of waterborne disease having multiple patches was also studied. Tuite *et al*. [36] proposed a gravity model to predict the sequence and timing of regional cholera epidemics in Haiti (2010) and suggested that adaptive strategies for vaccination may provide a modest reduction in morbidity and mortality in the economically challenged country. Collins *et al*. [37] studied the effect of heterogeneity in transmission due to socioeconomic status on the dynamics of waterborne diseases. Even though all the aforementioned studies have contributed immensely to improving the understanding of waterborne disease dynamics, other pathogen reservoirs that cause waterborne disease outbreaks have not been studied. In this paper, we address this research gap by formulating an appropriate mathematical epidemiological model that incorporates open dumpsites.

Another important issue of interest is the study of globally asymptotic properties of epidemiological models. This can help design effective control strategies intended to permanently reduce pathogen spread, or even break the chain of disease transmission. Understanding transient phenomena in potential epidemiological scenarios can also be important. It can help to prevent transitory epidemics that are triggered by external perturbations to a system, in which endemic transmission is not possible. That is, the disease-free equilibrium (*DFE*) is globally asymptotically stable [38]. This results in the threshold value of epidemiological models, which is called the basic reproductive number and denoted by $\mathcal{R}_0$. The study conducted in [28] showed that estimates of $\mathcal{R}_0$ and the infectious period can be sensitive to the relative contributions of the different transmission pathways and the pathogen's lifetime in water. Further studies [2, 28, 37, 39, 40] and references (therein) confirmed that the sensitivity of $\mathcal{R}_0$ is relevant for dynamical studies of waterborne diseases because the basic life history and epidemiological traits remain uncertain for many waterborne pathogens.

Based on the above discussion, this paper proposes a compartmental mathematical model to study the health impact of water and sanitation service deficits on the spread of waterborne diseases. The paper is organized as follows. In Sect. 2, the model proposed by Tien and Earn [28] is modified by incorporating water and sanitation services together with open dumpsites. In Sect. 3, the proposed model is analyzed to gain insights into the mechanisms of waterborne disease transmission and the control measures for waterborne diseases. The existence and the number of equilibria are established. The threshold value of the proposed model is derived by using the next generation method. The global stabilities of equilibria are analyzed by constructing the suitable Lyapunov functions and using LaSalle's invariance principle. In Sect. 4, numerical simulations are illustrated to determine the appropriate parameter values used for the proposed model and to determine the parameters that are sensitive to disease prevalence and the impact of water and sanitation (WatSan) services. Finally, conclusions are given in Sect. 5.

2 System modeling

Individuals can be infected with waterborne disease if they come near to an open dumpsite and contact waste directly [13]. This is because pathogens in open dumpsites can get into water sources through leachate and contaminate unprotected groundwater sources, or through precipitation that washes into surface water [11, 12]. Improving WatSan services is an effective means of reducing the number of infected individuals and the number of people who die each year as a result of diarrhea [41]. An increase in WatSan services would reduce the incidence of WatSan-related diseases, such as enteric diarrheal disease (EDD). Therefore, the system modeling included open dumpsites as reservoirs of pathogens and WatSan services, namely, the drinking water supply (DWS), wastewater and sewage treatment (WST), and municipal solid waste management (MSW). To investigate the impact caused by WatSan deficits on individual health and the state of the environment, we modified the model presented by Tien and Earn [28] with the following assumptions. We assumed that disease transmission occurred through two pathways, namely, a direct transmission pathway (human-to-human) and an indirect transmission pathway (environment-to-human). The indirect transmission pathway was formulated based on the *SIR* epidemic model for monitoring the dynamics of the sub-populations of susceptible individuals ($S(t)$), infectious individuals ($I(t)$), and recovered individuals ($R(t)$), so that the total population at time t is $N(t) = S(t) + I(t) + R(t)$. The indirect transmission pathway consisted of the *SIR* epidemic model together with compartments W and D. W and D, respectively, represent pathogen concentration in water reservoirs and open dumpsites that are potential reservoirs of pathogens. Compartment D represents open dumpsites and other pathogen reservoirs that are not water reservoirs. Furthermore, to improve the WatSan services, let $0 \leq r_1 \leq 1$, $0 \leq r_2 \leq 1$, and $0 \leq r_3 \leq 1$ represent the ratio of people who receive DWS, WST, and MSW services, respectively, in a community. A flow diagram of the formulated model, the susceptible–infected–water–dumpsite–recovered (*SIWDR*) model, is depicted in Fig. 1. The dynamics of each sub-population in Fig. 1 are described next.

The number of susceptible individuals increases at the recruitment rate of μN, where μ is the birth rate (intrinsic growth rate). The birth rate is assumed to be equal to the natural death rate so that the population size N remains constant. Thus, the susceptible

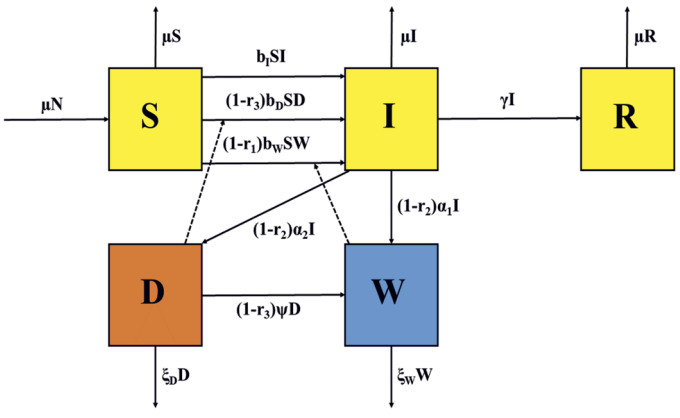

Figure 1 Compartment diagram for waterborne disease with the water and dumpsite–reservoir (SIWDR) model

Table 1 Description of state variables and units for SIWDR model (2.1)

State variables	Descriptions	Units
S	susceptible individual density	individuals km^{-2}
I	infected individual density	individuals km^{-2}
R	recovered individual density	individuals km^{-2}
W	pathogen concentration in water reservoir	cells ml^{-3}
D	pathogen concentration in dumpsite	cells kg^{-1}
N	total population density	individuals km^{-2}

Table 2 Description of model parameters and units for SIWDR model (2.1)

Parameters	Descriptions	Units
b_I	person–person contact rate	km^2 individuals^{-1} month^{-1}
b_W	reservoir–person contact rate	ml^3 cells^{-1} month^{-1}
b_D	dumpsite–person contact rate	kg cells^{-1} month^{-1}
γ^{-1}	infectious period	months
ξ_W^{-1}	pathogen lifetime in water reservoir	months
ξ_D^{-1}	pathogen lifetime in dumpsite	months
α_1	person–reservoir contact rate "shedding"	cells ml^{-3} month^{-1} km^2 individuals^{-1}
α_2	person–dumpsite contact rate	cells kg^{-1} month^{-1} km^2 individuals^{-1}
ψ	dumpsite–reservoir contact rate	kg ml^{-3} month^{-1}
μ	birth rate	month^{-1}
μ	non-disease-related death rate	month^{-1}
r_1	service coverage of DWS	–
r_2	service coverage of WST	–
r_3	service coverage of MSW	–

group decreases at the natural death rate μ. This includes when they contact infected individuals at a rate $b_I IS$, or through contact with contaminated water and infected waste at rates $(1 - r_1)b_W W$ and $(1 - r_3)b_D DS$, respectively. The parameters b_I, b_W, and b_D represent the transmission rate from person to person, water to person, and dumpsite to person contact, respectively. The number of infected individuals increases when these individuals generate secondary infections in two ways. The first way is through direct contact with susceptible individuals at a rate $b_I IS$. The second way is by first shedding the pathogen into water and solid waste compartments at rates $(1 - r_1)b_W WS$ and $(1 - r_3)b_D DS$, respectively. Susceptible individuals can subsequently come into contact with pathogens in these compartments. This population decreases at natural death rate μ. The recovered population increases when the infectious individuals recover from infection at rate γ and decreases at natural death rate μ.

The pathogen shedding rates from infected individuals into water and dumpsite compartments are given by $(1 - r_2)\alpha_1 I$ and $(1 - r_2)\alpha_2 I$, respectively. The pathogen shedding rate from the dumpsite compartment into the water compartment is given by $(1 - r_3)\psi D$. The parameters ξ_W and ξ_D give the decay rate of pathogens in the water and dumpsite compartments, respectively.

Therefore, based on the above descriptions and Fig. 1, the *SIWDR* model for the pathways of infection in waterborne diseases is given by the following deterministic system of

nonlinear differential equations:

$$\left.\begin{aligned}
\frac{dS}{dt} &= \mu N - (1-r_1)b_W SW - (1-r_3)b_D SD - b_I SI - \mu S,\\
\frac{dI}{dt} &= (1-r_1)b_W SW + (1-r_3)b_D SD + b_I SI - \gamma I - \mu I,\\
\frac{dW}{dt} &= (1-r_2)\alpha_1 I + (1-r_3)\psi D - \xi_W W,\\
\frac{dD}{dt} &= (1-r_2)\alpha_2 I - (1-r_3)\psi D - \xi_D D,\\
\frac{dR}{dt} &= \gamma I - \mu R,
\end{aligned}\right\} \tag{2.1}$$

where the descriptions of the model parameters and sample units in system (2.1) are given in Tables 1–2. Since the above model monitors human and pathogen populations, all associated parameters and state variables have nonnegative values.

3 Analysis of the model

3.1 Basic properties

Adding the first, second, and fifth equations of system (2.1) gives $dN/dt = 0$. Thus, the total human population N is constant. For convenience of analysis, we rewrite system (2.1) in terms of new dimensionless quantities by setting the state variables:

$$s = \frac{S}{N}, \qquad i = \frac{I}{N}, \qquad r = \frac{R}{N}, \qquad w = \frac{\xi_W}{\alpha_1 N}W, \qquad d = \frac{\xi_D}{\alpha_2 N}D,$$

so that

$$s + i + r = 1. \tag{3.1}$$

The model parameters are replaced by

$$\beta_I = b_I N, \qquad \beta_W = \frac{b_W \alpha_1 N}{\xi_W}, \quad \text{and} \quad \beta_D = \frac{b_D \alpha_2 N}{\xi_D}.$$

Using the expression above, system (2.1) is reduced to

$$\left.\begin{aligned}
s'(t) &= \mu - (1-r_1)\beta_W sw - (1-r_3)\beta_D sd - \beta_I si - \mu s,\\
i'(t) &= (1-r_1)\beta_W sw + (1-r_3)\beta_D sd + \beta_I si - \gamma i - \mu i,\\
w'(t) &= \xi_W(1-r_2)i + \frac{(1-r_3)\alpha_2 \xi_W \psi}{\alpha_1 \xi_D}d - \xi_W w,\\
d'(t) &= \xi_D(1-r_2)i - \big((1-r_3)\psi + \xi_D\big)d,
\end{aligned}\right\} \tag{3.2}$$

where $r = 1 - s - i$. This allows us to solve system (2.1) by studying system (3.2). Clearly, $\lim_{t\to\infty} \sup(s + i) \le 1$ implies $\lim_{t\to\infty} \sup(i(t)) \le 1$. It follows from the fourth equation of (3.2) that

$$d'(t) \le \xi_D(1-r_2) - \big((1-r_3)\psi + \xi_D\big)d,$$

which implies $\lim_{t\to\infty}\sup(d(t)) \le \frac{\xi_D(1-r_2)}{(1-r_3)\psi+\xi_D}$. Thus, from the third equation of system (3.2), we have

$$\begin{aligned} w' &\le \xi_W(1-r_2) + \frac{(1-r_3)\alpha_2\xi_W\psi}{\alpha_1\xi_D}\left(\frac{\xi_D(1-r_2)}{(1-r_3)\psi+\xi_D}\right) - \xi_W w \\ &= \xi_W(1-r_2)\left(1+\frac{(1-r_3)\alpha_2\psi}{\alpha_1((1-r_3)\psi+\xi_D)}\right) - \xi_W w. \end{aligned}$$

It is easy to show that

$$\lim_{t\to\infty}\sup\bigl(w(t)\bigr) \le (1-r_2)\left(1+\frac{(1-r_3)\alpha_2\psi}{\alpha_1((1-r_3)\psi+\xi_D)}\right).$$

Hence, the feasible region

$$\Omega = \bigl\{(s,i,w,d) : 0 \le s+i \le 1, w \le w_c, \text{and } d \le d_c\bigr\}$$

is positively invariant for model (3.2) with $w_c = (1-r_2)(1+\frac{(1-r_3)\alpha_2\psi}{\alpha_1((1-r_3)\psi+\xi_D)})$ and $d_c = \frac{\xi_D(1-r_2)}{(1-r_3)\psi+\xi_D}$. Thus, the existence, uniqueness, and continuation results for model (3.2) hold in Ω. All solutions that start in Ω remain in Ω for all $t \ge 0$ [42]. Hence, model (3.2) is mathematically and epidemiologically well posed, and it is sufficient to consider the dynamics of the flow generated by model (3.2) in Ω.

3.2 Disease-free equilibrium and basic reproductive number

3.2.1 Local stability

In the absence of infection and with adequate water and sanitation services ($i = 0$, $w = 0$ and $d = 0$), system (3.2) has a unique disease-free equilibrium (DFE) denoted by

$$\varepsilon_0\bigl(s^0, i^0, w^0, d^0\bigr) = (1,0,0,0). \tag{3.3}$$

According to the next generation matrix and using the notation in [43], system (3.2) is rewritten as

$$x'(t) = \mathcal{F} - \bigl(\mathcal{V}^- - \mathcal{V}^+\bigr), \tag{3.4}$$

where $x = (i,w,d,s)^T$,

$$\mathcal{F} = \begin{pmatrix} \tilde{r}_1\beta_W sw + \tilde{r}_3\beta_D sd + \beta_I si \\ 0 \\ 0 \\ 0 \end{pmatrix},$$

$$\mathcal{V}^- = \begin{pmatrix} \gamma i + \mu i \\ \xi_W w \\ (\tilde{r}_3\psi + \xi_D)d \\ Q_1 \end{pmatrix}, \qquad \mathcal{V}^+ = \begin{pmatrix} 0 \\ \xi_W\tilde{r}_2 i + \frac{Q_2}{\alpha_1\xi_D}d \\ \xi_D\tilde{r}_2 i \\ \mu \end{pmatrix}$$

with $Q_1 = \tilde{r}_1\beta_W sw + \tilde{r}_3\beta_D sd + \beta_I si + \mu s$ and $Q_2 = \tilde{r}_3\alpha_2\xi_W\psi$, respectively. Clearly, $x_0 = (0,0,0,1)$ is a disease-free equilibrium of system (3.4), which is identical to ε_0 of system

(3.2). It is easy to show that system (3.4) satisfies assumptions (A1)–(A5) in [43]. Further, the derivatives $D\mathcal{F}(x_0)$ and $D\mathcal{V}(x_0)$ are partitioned as

$$D\mathcal{F}(x_0) = \begin{pmatrix} F & 0 \\ 0 & 0 \end{pmatrix} \quad \text{and} \quad \begin{pmatrix} V & 0 \\ J_3 & J_4 \end{pmatrix},$$

where the matrices F (for the new infection terms) and V (for the transition terms) are given, respectively, by

$$F = \begin{pmatrix} \beta_I & \tilde{r}_1\beta_W & \tilde{r}_3\beta_D \\ 0 & 0 & 0 \\ 0 & 0 & 0 \end{pmatrix} \quad \text{and} \quad V = \begin{pmatrix} \gamma+\mu & 0 & 0 \\ -\xi_W\tilde{r}_2 & \xi_W & -\frac{\tilde{r}_3\alpha_2\xi_W\psi}{\alpha_1\xi_D} \\ -\xi_D\tilde{r}_2 & 0 & \tilde{r}_3\psi+\xi_D \end{pmatrix}, \tag{3.5}$$

where $\tilde{r}_1 = 1-r_1$, $\tilde{r}_2 = 1-r_2$, and $\tilde{r}_3 = 1-r_3$. Defining $\mathcal{R}_0 = \rho(FV^{-1})$, where ρ is the spectral radius of matrix FV^{-1}, we get

$$\mathcal{R}_0 = \frac{\alpha_1(\tilde{r}_3\psi+\xi_D)(\beta_I+\tilde{r}_1\tilde{r}_2\beta_W)+\tilde{r}_2\tilde{r}_3(\alpha_1\beta_D\xi_D+\tilde{r}_1\alpha_2\beta_W\psi)}{\alpha_1(\mu+\gamma)(\psi\tilde{r}_3+\xi_D)}. \tag{3.6}$$

According to Theorem 1 in [43], the following result is established.

Lemma 3.1 *The DFE ε_0 of system (3.2) is locally asymptotically stable* (LAS) *if $\mathcal{R}_0 < 1$ and unstable if $\mathcal{R}_0 > 1$.*

The local stability that resulted in Lemma 3.1 implies that for $\mathcal{R}_0 < 1$ the disease dies out and for $\mathcal{R}_0 > 1$ the infected population is not reduced to zero. Thus, the quality that $\mathcal{R}_0 > 1$ is the threshold value of model (3.2). Furthermore, the result in Lemma 3.1 verifies that if the initial sizes of the sub-groups of the model are within the basin of attraction of ε_0, the total number of infected people in the population can be reduced to zero whenever $\mathcal{R}_0 < 1$. Moreover, it was found that the value of $\mathcal{R}_0$ depends on the ratios of people who receive the DWS, WST, and MSW services: r_1, r_2, and r_3, respectively. This theoretical determination of conditions of these ratios can make $\mathcal{R}_0$ independent of the initial sizes of the five state variables. This is of great public health interest, which is later illustrated by analyzing the global stability.

3.2.2 Global stability of DFE

We claim the following result.

Theorem 3.2 *The DFE ε_0 of model (3.2) is globally asymptotically stable* (GAS) *in Ω if $\mathcal{R}_0 < 1$.*

Proof We introduce a new function

$$L = i + \mathcal{A}_W w + \mathcal{A}_D d,$$

where $\mathcal{A}_W = \frac{\tilde{r}_1\beta_W}{\xi_W}$ and $\mathcal{A}_D = \frac{\tilde{r}_3(\alpha_1\beta_D\xi_D+\tilde{r}_1\alpha_2\beta_W\psi)}{\alpha_1\xi_D(\psi\tilde{r}_3+\xi_D)}$. The derivative of L with the solutions of (3.2) is

$$\begin{aligned} L'(t) &= (s-1)(\tilde{r}_1\beta_W w + \tilde{r}_3\beta_D d) \\ &\quad + (\mu+\gamma)\left(\frac{\tilde{r}_2\tilde{r}_3(\alpha_1\beta_D\xi_D + \tilde{r}_1\alpha_2\beta_W\psi) + \alpha_1(\tilde{r}_3\psi + \xi_D)(\beta_I s + \tilde{r}_1\tilde{r}_2\beta_W)}{\alpha_1(\mu+\gamma)(\psi\tilde{r}_3 + \xi_D)} - 1\right) i \\ &\leq (\mu+\gamma)(\mathcal{R}_0 - 1)i. \end{aligned}$$

It is obvious that $L'(t) \leq 0$ if $\mathcal{R}_0 \leq 1$. Furthermore, $L'(t) = 0$ if $i = 0$. The Lyapunov–LaSalle theorem [44] implies that all paths in Ω approach the largest positively invariant subset of set $\{(s,i,d,w)|i=0\}$. On the boundary of Ω, where $i = 0$, we have $r'(t) = -\mu r$, so $r = r(0)e^{-\mu t} \to 0$ as $t \to \infty$, and $d'(t) = -(\tilde{r}_3\psi + \xi_D)d$. Then $d(t) = d(0)e^{-(\tilde{r}_3\psi+\xi_D)t} \to 0$ as $t \to \infty$. Thus, we easily obtain $\lim_{t\to\infty} w(t) = 0$. Hence, all solution paths in Ω approach the DFE ε_0. This completes the proof of this theorem. □

3.3 Endemic equilibrium (EE)

In the presence of infection ($i \neq 0$) and insufficient water and sanitation services ($w \neq 0$ and $d \neq 0$), model (3.2) has a unique EE, which is given by $\varepsilon_1 = (s^*, i^*, w^*, d^*, r^*)$ where:

$$\left.\begin{aligned} s^* &= \frac{1}{\mathcal{R}_0}, \qquad i^* = \frac{\mu}{(\mu+\gamma)\mathcal{R}_0}(\mathcal{R}_0 - 1), \qquad d^* = \left(\frac{\tilde{r}_2\xi_D}{\tilde{r}_3\psi + \xi_D}\right)i^*, \\ w^* &= \left(\frac{\tilde{r}_2\alpha_1(\tilde{r}_3\psi + \xi_D) + \tilde{r}_2\tilde{r}_3\alpha_2\psi}{\alpha_1(\tilde{r}_3\psi + \xi_D)}\right)i^*. \end{aligned}\right\} \tag{3.7}$$

Clearly, $i^* > 0$ (corresponding to the EE, see (3.7) whenever $\mathcal{R}_0 > 1$, $i^* = 0$ when $\mathcal{R}_0 = 1$ (corresponding to the DFE, see (3.3)) and $i^* < 0$ (meaningless) whenever $\mathcal{R}_0 < 1$.

3.3.1 Local stability

Linearizing model (3.2) around its unique EE is analyzed by the use of the center manifold theory [45] as described in Theorem 4.1 [46]. The following theorem, thus, is established.

Theorem 3.3 *The unique* EE ε_1 *of the model* (3.2) *is LAS if* $\mathcal{R}_0 > 1$ *and is close to* 1.

Proof The Jacobian of system (3.2) evaluated at ε_0 is given by

$$J(\varepsilon_0) = \begin{bmatrix} -\mu & -\beta_I & -\tilde{r}_1\beta_W & -\tilde{r}_3\beta_D \\ 0 & \beta_W - (\mu+\gamma) & \tilde{r}_1\beta_W & \tilde{r}_3\beta_D \\ 0 & \tilde{r}_2\xi_W & -\xi_W & \frac{\tilde{r}_3\alpha_2\xi_W\psi}{\alpha_1\xi_D} \\ 0 & \tilde{r}_2\xi_D & 0 & -(\tilde{r}_3 + \xi_D) \end{bmatrix}.$$

Suppose, that $\beta_I = \beta_I^*$ is a bifurcation parameter. Solving $\mathcal{R}_0 = 1$ for β_I gives

$$\beta_I^* = (\gamma+\mu) - \frac{\tilde{r}_2(\tilde{r}_1\beta_W(\tilde{r}_3\alpha_2\psi + \alpha_1(\tilde{r}_3\psi + \xi_D)) + \tilde{r}_3\alpha_1\beta_D\xi_D)}{\alpha_1(\tilde{r}_3\psi + \xi_D)}.$$

It was found that system (3.2) with $\beta_I = \beta_I^*$ has at least one non-hyperbolic equilibrium point. Thus, the centre manifold theory [45] as described in Theorem 4.1 [46] is used to

analyze the LAS of EE ε_1 of the system (3.2) with $\beta_I = \beta_I^*$. The right eigenvector of $J(\beta_I^*)$ with $\beta_I = \beta_I^*$ is given by $w = [w_1, w_2, w_3, w_4, w_5]^T$, where

$$w_1 = -\frac{(\gamma+\mu)(\tilde{r}_3\psi+\xi_D)w_4}{\tilde{r}_2\mu\xi_D}, \qquad w_2 = \frac{(\tilde{r}_3\psi+\xi_D)w_4}{\tilde{r}_2\xi_D},$$
$$w_3 = \frac{(\alpha_1(\tilde{r}_3\psi+\xi_D)+\tilde{r}_3\alpha_2\psi)w_4}{\alpha_1\xi_D}, \quad \text{and} \quad w_4 > 0.$$

Further, $J(\beta_I^*)$ with $\beta_I = \beta_I^*$ has a left eigenvector $v = [v_1, v_2, v_3, v_4, v_5]$, where

$$v_1 = v_5 = 0, \qquad v_3 = \frac{\tilde{r}_1\beta_W v_2}{\xi_W}, \qquad v_4 = \frac{\tilde{r}_3(\alpha_1\beta_D\xi_D+\tilde{r}_1\alpha_2\psi\beta_W)v_2}{\alpha_1\xi_D(\tilde{r}_3\psi+\xi_D)}, \quad \text{and}$$
$$v_2 > 0.$$

For system (3.2), the associated non-zero partial derivatives of the function $f_i(s,i,w,d,r)$, $i = 1,\dots,5$ on the right-hand side of each equation are given by

$$\frac{\partial^2 f_1}{\partial x_1\partial x_2} = \frac{\partial^2 f_1}{\partial x_2\partial x_1} = -\beta_I^*, \qquad \frac{\partial^2 f_1}{\partial x_1\partial x_3} = \frac{\partial^2 f_1}{\partial x_3\partial x_1} = -\tilde{r}_1\beta_W,$$
$$\frac{\partial^2 f_1}{\partial x_1\partial x_4} = \frac{\partial^2 f_1}{\partial x_4\partial x_1} = -\tilde{r}_3\beta_D, \qquad \frac{\partial^2 f_2}{\partial x_1\partial x_2} = \frac{\partial^2 f_2}{\partial x_2\partial x_1} = \beta_I^*,$$
$$\frac{\partial^2 f_2}{\partial x_1\partial x_3} = \frac{\partial^2 f_2}{\partial x_3\partial x_1} = \tilde{r}_1\beta_W, \qquad \frac{\partial^2 f_2}{\partial x_1\partial x_4} = \frac{\partial^2 f_2}{\partial x_4\partial x_1} = \tilde{r}_3\beta_D,$$
$$\frac{\partial^2 f_1}{\partial x_2\partial\beta_I^*} = -1, \qquad \frac{\partial^2 f_2}{\partial x_2\beta_I^*} = 1,$$

for variables $x_1 = s$, $x_2 = i$, $x_3 = w$, and $x_4 = d$.

Using the above expressions, parameters a and b as given in Theorem 4.1 [46] are computed.

$$a = \sum_{k,i,j=1}^{5} v_k w_i w_j \frac{\partial^2 f_k}{\partial x_i\partial x_j}(0,0)$$
$$= -\frac{2v_2w_4^2\mathcal{C}_1\mathcal{C}_2(\alpha_1\mathcal{C}_1(\beta_I+\tilde{r}_1\tilde{r}_2\beta_W)+\tilde{r}_2\tilde{r}_3(\alpha_1\beta_D\xi_D+\tilde{r}_1\alpha_2\beta_W\psi))}{\mu\alpha_1(\tilde{r}_2\xi_D)^2},$$

and

$$b = \sum_{k,i=1}^{5} v_k w_i \frac{\partial^2 f_k}{\partial x_i\partial\phi}(0,0) = \frac{\mathcal{C}_1 v_2 w_4}{\tilde{r}_2\xi_D},$$

where $\mathcal{C}_1 = \tilde{r}_3\psi + \xi_D$ and $\mathcal{C}_2 = \gamma + \mu$. Clearly, $a < 0$ and $b > 0$. Hence, by Theorem 4.1 in [46], the unique EE ε_1 of the system (3.2) exists and is LAS whenever $\mathcal{R}_0 > 1$ and $\beta_I^* < \beta_I$ with β_I close to β_I^*. □

This theorem indicates that if $\mathcal{R}_0 > 1$, the EE ε_1 is locally asymptotically stable (that is, the disease will persist in the community if the initial sizes of the four-state variables are within the vicinity of ε_1). If the EE ε_1 is globally asymptotically stable, then any trajectories

tend toward the attractor of ε_1, of system (3.2), regardless of the initial conditions. This means that the attracting basin of trajectories in the dynamical system is the state space [47]. In a biological sense, this property gives the theoretical determination of conditions that can cause $\mathcal{R}_0 > 1$, irrespective of the initial sizes of the five state variables that increase the risk of a disease outbreak. The Lyapunov function is constructed and LaSalle's invariance principle, which is the criterion for the asymptotic stability of an autonomous dynamical system [48–51], is applied to prove the global stability of ε_1. The following theorem, therefore, is established.

Theorem 3.4 *The unique* EE ε_1 *of model* (3.2) *is globally asymptotically stable* (*GAS*) *in* Ω *whenever* $\mathcal{R}_0 > 1$.

Proof Consider the Lyapunov function

$$V(t) = A_1\left(s - s^* - s^* \ln\left(\frac{s}{s^*}\right) + i - i^* - i^* \ln\left(\frac{i}{i^*}\right)\right) + \frac{1}{\xi_W}\left(w - w^* - w^* \ln\left(\frac{w}{w^*}\right)\right) + A_2\left(d - d^* - d^* \ln\left(\frac{d}{d^*}\right)\right),$$

where

$$A_1 = \frac{\tilde{r}_2}{\tilde{r}_1\beta_W w^* s^*}\left(i^* + \frac{\tilde{r}_3\alpha_2\psi}{\tilde{r}_2\alpha_1\xi_D}d^*\right),$$
$$A_2 = \frac{\tilde{r}_3 d^*}{\tilde{r}_2\xi_D i^*}\left(\frac{\alpha_2\psi}{\alpha_1\xi_D} + \frac{\tilde{r}_2\beta_D i^*}{\tilde{r}_1\beta_W w^*} + \frac{\tilde{r}_3\alpha_2\psi\beta_D d^*}{\tilde{r}_1\alpha_1\xi_D\beta_W w^*}\right).$$

The derivative of $V(t)$ and the solutions of system (3.2) are given by

$$\begin{aligned}\frac{dV}{dt} &= A_1\left(1 - \frac{s^*}{s}\right)(\mu - \tilde{r}_1\beta_W sw - \tilde{r}_3\beta_D sd - \beta_I si - \mu s)\\ &\quad + A_1\left(1 - \frac{i^*}{i}\right)(\tilde{r}_1\beta_W sw + \tilde{r}_3\beta_D sd + \beta_I si - \gamma i - \mu i)\\ &\quad + \xi_W\left(1 - \frac{w^*}{w}\right)\left(\tilde{r}_2 i + \frac{\tilde{r}_3\alpha_2\psi}{\alpha_1\xi_D}d - w\right)\\ &\quad + A_2\left(1 - \frac{d^*}{d}\right)\left(\xi_D\tilde{r}_2 i - (\tilde{r}_3\psi + \xi_D)d\right).\end{aligned} \tag{3.8}$$

At steady state when $\mathcal{R}_0 > 1$, and from the first four equations of system (3.2), we have

$$\left.\begin{aligned}\mu &= \tilde{r}_1\beta_W s^* w^* + \tilde{r}_3\beta_D s^* d^* + \beta_I s^* i^* + \mu s^*,\\ (\gamma + \mu)i^* &= \tilde{r}_1\beta_W s^* w^* + \tilde{r}_3\beta_D s^* d^* + \beta_I s^* i^*,\\ w^* &= \tilde{r}_2 i^* + \frac{\tilde{r}_3\alpha_2\psi}{\alpha_1\xi_D}d^*,\\ (\tilde{r}_3\psi + \xi_D)d^* &= \xi_D\tilde{r}_2 i^*.\end{aligned}\right\} \tag{3.9}$$

Substituting expressions (3.9) into (3.8) and rearranging give

$$\begin{aligned}
\frac{dV}{dt} &= A_1\left(\beta_I s^* i^* + \mu s^*\right)\left(2 - \frac{s^*}{s} - \frac{s}{s^*}\right) \\
&\quad + A_1\tilde{r}_1\beta_W s^* w^*\left(2 + \frac{w}{w^*} - \frac{s^*}{s} - \frac{i}{i^*} - \frac{si^*w}{s^*iw^*}\right) \\
&\quad + A_1\tilde{r}_3\beta_D s^* d^*\left(3 - \frac{s^*}{s} - \frac{si^*d}{s^*id^*} - \frac{id^*}{i^*d}\right) \\
&\quad + \tilde{r}_2 i^*\left(1 + \frac{i}{i^*} - \frac{w}{w^*} - \frac{iw^*}{i^*w}\right) \\
&\quad + \frac{\tilde{r}_3\alpha_2\psi d^*}{\xi_D\alpha_1}\left(2 + \frac{i}{i^*} - \frac{w}{w^*} - \frac{w^*d}{wd^*} - \frac{id^*}{i^*d}\right) \\
&= A_1\left(\beta_I s^* i^* + \mu s^*\right)\left(2 - \frac{s^*}{s} - \frac{s}{s^*}\right) \\
&\quad + A_1\tilde{r}_3\beta_D s^* d^*\left(3 - \frac{s^*}{s} - \frac{si^*d}{s^*id^*} - \frac{id^*}{i^*d}\right) \\
&\quad + \tilde{r}_2 i^*\left(3 - \frac{s^*}{s} - \frac{si^*w}{s^*iw^*} - \frac{iw^*}{i^*w}\right) \\
&\quad + \frac{\tilde{r}_3\alpha_2\psi d^*}{\xi_D\alpha_1}\left(4 - \frac{s^*}{s} - \frac{si^*w}{s^*iw^*} - \frac{w^*d}{wd^*} - \frac{id^*}{i^*d}\right).
\end{aligned}$$

It follows from the arithmetic mean is greater than or equal to the geometric mean that the following inequalities hold:

$$\left.\begin{aligned}
&2 - \frac{s^*}{s} - \frac{s}{s^*} \le 0, \\
&3 - \frac{s^*}{s} - \frac{si^*d}{s^*id^*} - \frac{id^*}{i^*d} \le 0, \\
&3 - \frac{s^*}{s} - \frac{si^*w}{s^*iw^*} - \frac{iw^*}{i^*w} \le 0, \\
&4 - \frac{s^*}{s} - \frac{si^*w}{s^*iw^*} - \frac{w^*d}{wd^*} - \frac{id^*}{i^*d} \le 0,
\end{aligned}\right\} \tag{3.10}$$

for $s \ge 0$, $i \ge 0$, $d \ge 0$, $w \ge 0$. Using the inequalities in (3.10) and that all the model parameters are nonnegative, it is clear that $dV/dt \le 0$ whenever $\mathcal{R}_0 > 1$. Furthermore, $dV/dt = 0$ if and only if $s = s^*$, $i = i^*$, $d = d^*$, and $w = w^*$. Hence, $V(t)$ is a Lyapunov function in Ω. By LaSalle's invariance principle [52], it is found that $s \to s^*$, $i \to i^*$, $d \to d^*$, and $w \to w^*$ as $t \to \infty$. Hence, the EE (ε_1) of model (3.2) is GAS. That is, every solution of model (3.2) with initial condition in Ω approaches ε_1 as $t \to \infty$ whenever $\mathcal{R}_0 > 1$. □

4 Numerical simulations

4.1 Estimation values of model parameters

From the outbreak size of cholera in Haiti in 2010, the death toll was approximately 9,700, and there were over 800,000 suspected cases [53]. Model (3.2) used this cholera outbreak as a case study. The model was simulated with N = 2,200,000, which is the approximate population in the capital of Haiti in 2010 [54]. The parameter values are given in Table 3 for

Table 3 Parameters values used in model (3.2)

Parameters	Nominal values	Ranges	Sources
μ	0.00005363	0–0.0012	[55, 56]
β_I	0.43	0.3–3	[29, 36]
β_W	9.49	0.0003–30	[29, 36, 57]
β_D	6.54	0.0003–30	[29, 36, 57]
γ	12.10	1.5–30	[29, 36, 58, 59]
α_1	3.89	0.3–300	[57, 58, 60]
α_2	19.93	0.3–300	[57, 58, 60]
ψ	11.32	0.3–300	[57, 58, 60]
ξ_W	2.63	0.6857–10	[36, 57]
ξ_D	2.58	0.3477–12	[61]
r_1	0.635	0.0–1.0	[62, 63]
r_2	0.225	0.0–1.0	[62, 63]
r_3	0.1	0.0–1.0	[64]

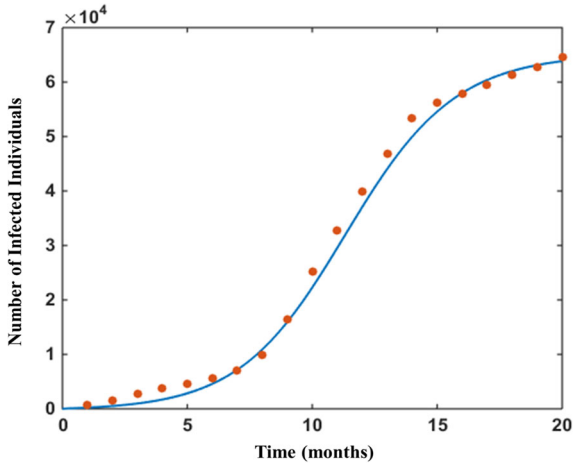

Figure 2 Comparison of the cumulative predicted infection data produced by model (3.2) and the cumulative real data from Haiti, 2010 [65]. Red points denote real data and the blue line denotes predicted data

predicting the number of infected individuals. The results are then used to compute the cumulative number of predicted infected individuals by solving the differential equation

$$\frac{dC}{dt} = kI, \tag{4.1}$$

where $k = 0.99$ is the rate of progression in the monthly infectious state. With all values given in Table 3, the basic reproductive number is $\mathcal{R}_0 = 1.2406$, which is within the range $(1.06, 2.78)$ [36, 66]. This value indicates that cholera persists in the community and can result in a disease outbreak, as guaranteed by Theorem 3.4. As shown in Fig. 2, the cumulative predicted data are compared with the cumulative real cholera data in Haiti 2010, which are reported by the Pan American Health Organization (PAHO) [65]. Figure 2 shows that the cumulative predicted data produced by model (3.2) are close to the real data generated by using a statistical measure, the coefficient of determination, $R^2 = 0.9946$. This study result verifies that model (3.2) can be used to investigate the cholera transmission in Haiti (2010). Moreover, the values of model parameters given in Table 3 are appropri-

ate for model (3.2). These values are used to investigate the influential factors that can mitigate the 2010 cholera outbreak in Haiti in the next sections.

4.2 Sensitivity analysis of the basic reproductive number

Sensitivity analysis [67] is a tool for determining the relative importance of the different factors responsible for disease transmission. The initial disease transmission is directly related to the basic reproductive number $\mathcal{R}_0$. We computed the sensitivity indices of $\mathcal{R}_0$ in a model with parameter p, defined by using partial derivatives

$$\Upsilon_p^{\mathcal{R}_0} = \frac{\partial \mathcal{R}_0}{\partial p} \times \frac{p}{\mathcal{R}_0}. \tag{4.2}$$

Table 4 shows the order of sensitivity indices of $\mathcal{R}_0$ in relation to thirteen model parameters, evaluated at the baseline values given in Table 3. The values are arranged from the most to the least sensitive parameters. A negative value means that increasing a model parameter value decreases the value of $\mathcal{R}_0$, resulting in a decrease in the infected individual density. In contrast, a positive value means that increasing a model parameter value increases the value of $\mathcal{R}_0$, resulting in an increase in the infected individual density. The model parameters (β_W, α_1, α_2, ψ, β_D, β_I) affect the increase in the initial transmission, and β_W is the most sensitive parameter. In contrast, the model parameters (r_1, γ, r_2, r_3, ξ_W, ξ_D, μ) affect the decrease in the initial disease transmission, and r_1 is the most sensitive parameter. Regarding the coverage of DWS, WST, and MSW services, the coverage of DWS service (r_1) is the most sensitive parameter, followed by the coverage of WST service (r_2) and the coverage of MSW service (r_3). This result indicates that improving the coverage of the DWS service is the most effective intervention to control a waterborne disease outbreak.

Although an increase in the coverage of DWS is the most effective strategy, choosing only one strategy to control a waterborne outbreak might not be an effective strategy. Next, the results of combining two of these model parameters on the value of $\mathcal{R}_0$ are explored using the contour plots of $\mathcal{R}_0$ (see Fig. 3). The results show that an increase in the coverage r_1, r_2, and r_3 services decreases the value of $\mathcal{R}_0$ to be less than unity. However, it is observed that if the coverage of r_1 is 0.65, the coverage of r_2 should be increased by at least 0.38 (compared to the baseline value $r_2 = 0.225$) to decrease $\mathcal{R}_0$ to be less than 1 (see

Table 4 Sensitivity indices of $\mathcal{R}_0$ to model parameters for model (3.2), evaluated at the baseline parameter values given in Table 3

Model parameters	Sensitivity indices $\Upsilon_p^{\mathcal{R}_0}$
r_1	−1.5831
γ	−1.0000
β_W	0.9099
α_1	0.7311
α_2	0.7311
r_2	−0.2820
r_3	−0.2820
ψ	0.0987
ξ_W	−0.0987
ξ_D	−0.0987
β_D	0.0614
β_I	0.0286
μ	-4.4322×10^{-6}

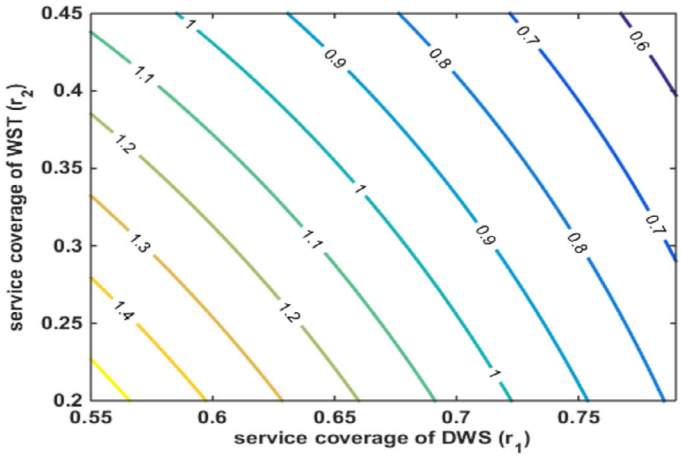

(a) $\mathcal{R}_0 = \mathcal{R}_0(r_1, r_2)$

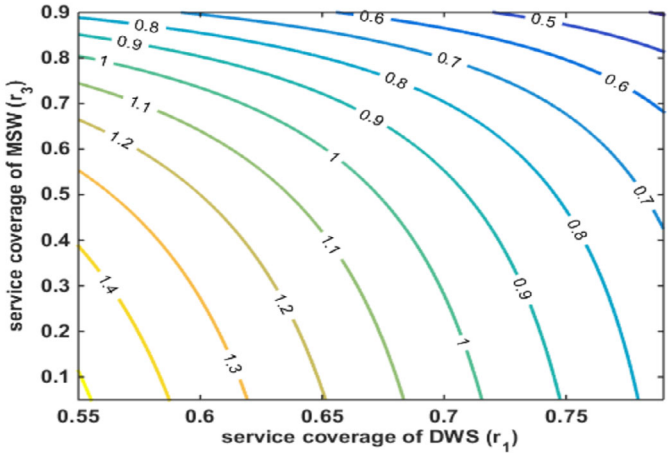

(b) $\mathcal{R}_0 = \mathcal{R}_0(r_1, r_3)$

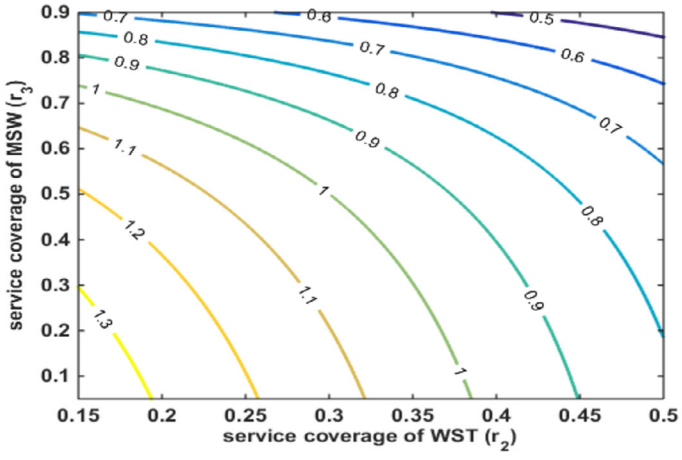

(c) $\mathcal{R}_0 = \mathcal{R}_0(r_2, r_3)$

Figure 3 Contour plots of the surface $\mathcal{R}_0$ as the function of the services coverage r_1, r_2, and r_3. The values of the other model parameters are given in Table 2

Fig. 3(a)). In this case, an increase in the coverage of the r_3 service has the least impact in decreasing the value of $\mathcal{R}_0$ (see Figs. 3(b) and 3(c)). In summary, this study suggests that the WatSan services coverage would be a crucial factor to mitigate the health impact of the 2010 cholera outbreak in Haiti.

Generally, coverages of DWS, WST, and MSW services can decrease the initial disease transmission and interrupt the transmission of waterborne diseases.

4.3 Impacts of WatSan services

The 2013–2022 plan to combat cholera in Haiti has been put in place [68]. The plan is to spend approximately $1.6 billion U.S. dollars to improve WatSan service coverage. The budget allocation for improving the coverage of DWS, WST, and MSW services was set to be 49.5%, 28.1%, and 22.4%, respectively. This budget allocation satisfies the result obtained in Sect. 4.2. Our research results show that the coverage of DWS, WST, and MSW services significantly impacts the control of waterborne diseases.

In 2010, the government proposed that every citizen must have improved water supplies and sanitation services. However, only 1.5% of water supplies and only 12.5% of sanitation facilities improved from 2010 to 2017. According to the 2017 UNICEF report [69], the proportion of the Haitian population with improved water supplies and sanitation services was only 65% and 35% of the total population, respectively. In Haiti, the progress of WatSan service improvement was not done according to the 10-year plan proposed by the Haitian government [68]. Therefore, insufficient WatSan service provisions were likely the cause of the persistent cholera outbreaks in Haiti.

In this section, the impacts of improving WatSan services are investigated as strategies to interrupt the transmission pathways of a cholera outbreak. Model (3.2) was simulated to determine the fraction of infected individuals and the fraction of pathogens in water reservoirs and dumpsites with varying percentages of coverage of the DWS service (r_1), WST service (r_2), and MSW service (r_3). The other parameters used in the simulation are given in Table 2. The dynamic behavior of the fraction of infected individuals and the fraction of pathogens in water reservoirs and dumpsites is shown in Figs. 4–6.

From the 2010 cholera outbreak data in Haiti, we set the starting values of r_1, r_2, and r_3 to be 65%, 35%, and 10 %, respectively. The fraction of infected individuals (Figs. 4–6(top)) uses fixed values of two out of three of the other variables ($r_1 = 65\%$, $r_2 = 35\%$, or $r_3 = 10\%$). The lines in each graph show that a change in the coverage of DWS service (r_1) has the greatest impact in reducing the fraction of infected individuals. In Figs. 4–6(middle), the lines in each graph show that a change in the coverage of WST service (r_2) has the greatest impact in reducing the fraction of pathogens in water reservoirs. In Figs. 4–6(bottom), the lines in each graph show that a change in the coverage of WST service (r_2) has the greatest impact in reducing the fraction of pathogens in dumpsites. Figure 4 shows that the fraction of infected individuals, the fraction of pathogens in water reservoirs, and the fraction of pathogens in dumpsites decrease with an improvement in DWS service coverage. However, with a coverage of 65%, the outbreak seems to maintain a steady state of the fraction of infected individuals (noted by the blue horizontal line in Fig. 4(top)). Relatedly, the fraction of pathogens in water reservoirs and the fraction of pathogens in dumpsites (in this case) also seem to stay constant (noted by the blue horizontal line in Figs. 4(middle) and 4(bottom)). Note that with varying r_1, the peaks in Fig. 4(bottom) occur approximately at the same position. This is because changing the coverage of DWS service (r_1) does not

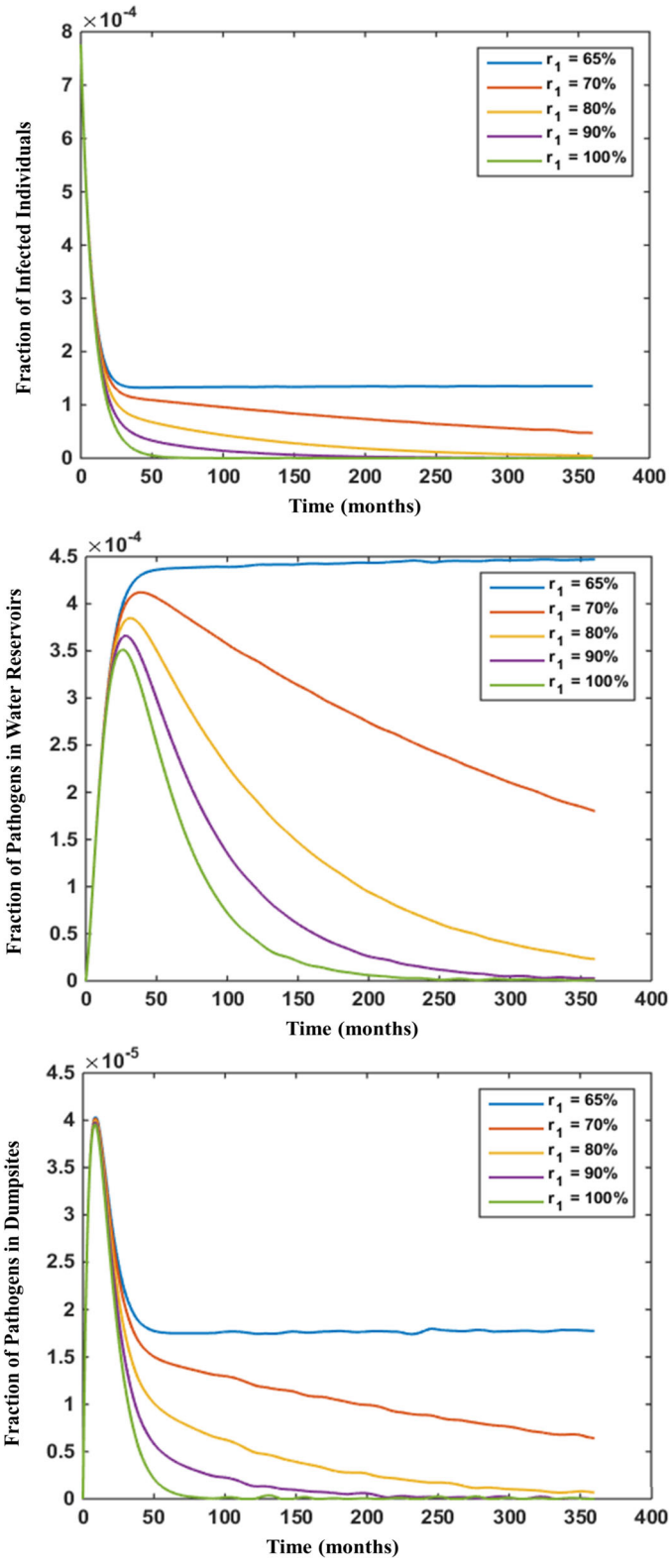

Figure 4 Dynamic behavior of the fraction of infected individuals (top), fraction of pathogens in water reservoirs (middle), and fraction of pathogens in dumpsites (bottom), with $r_2 = 35\%$, $r_3 = 10\%$, and varying r_1 from 65%, 70%, 80%, 90%, and 100%

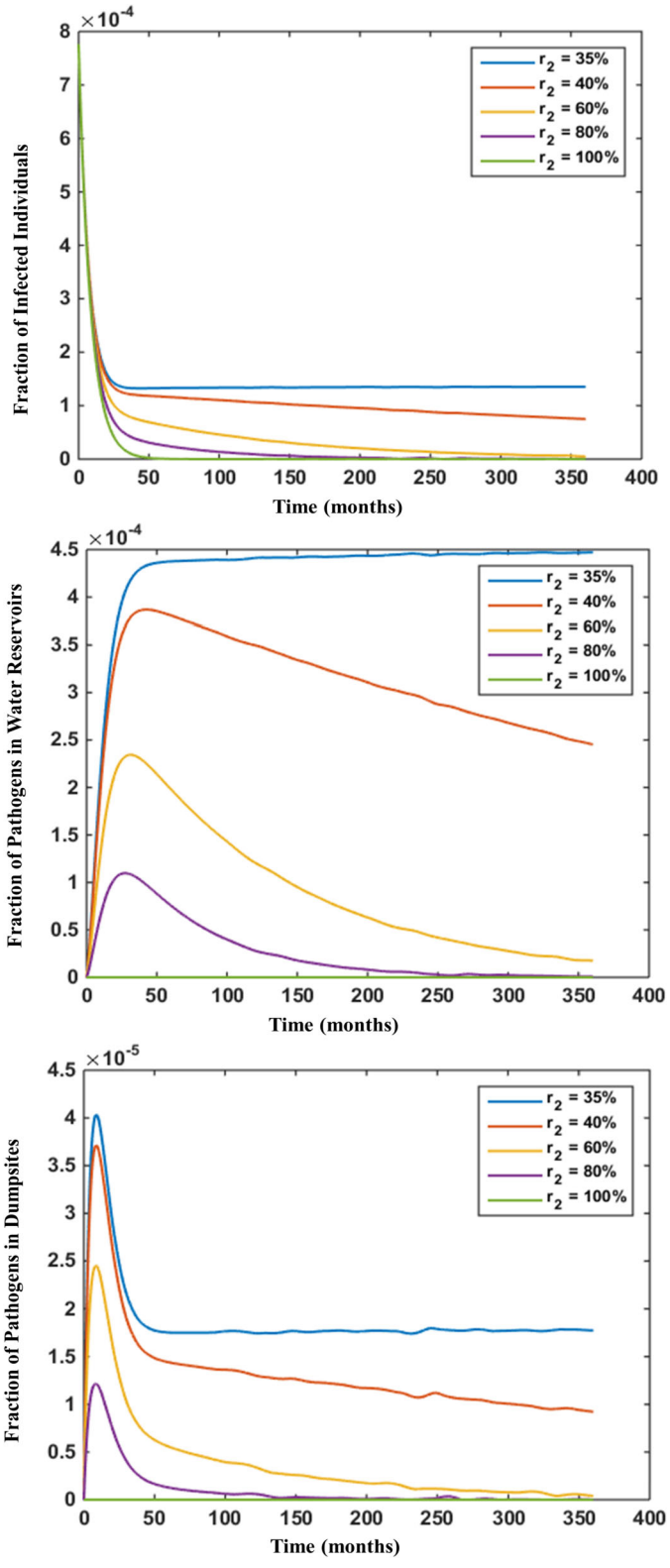

Figure 5 Dynamic behavior of the fraction of infected individuals (top), fraction of pathogens in water reservoirs (middle), and fraction of pathogens in dumpsites (bottom), with $r_1 = 65\%$, $r_3 = 10\%$, and varying r_2 from 35%, 40%, 60%, 80%, and 100%

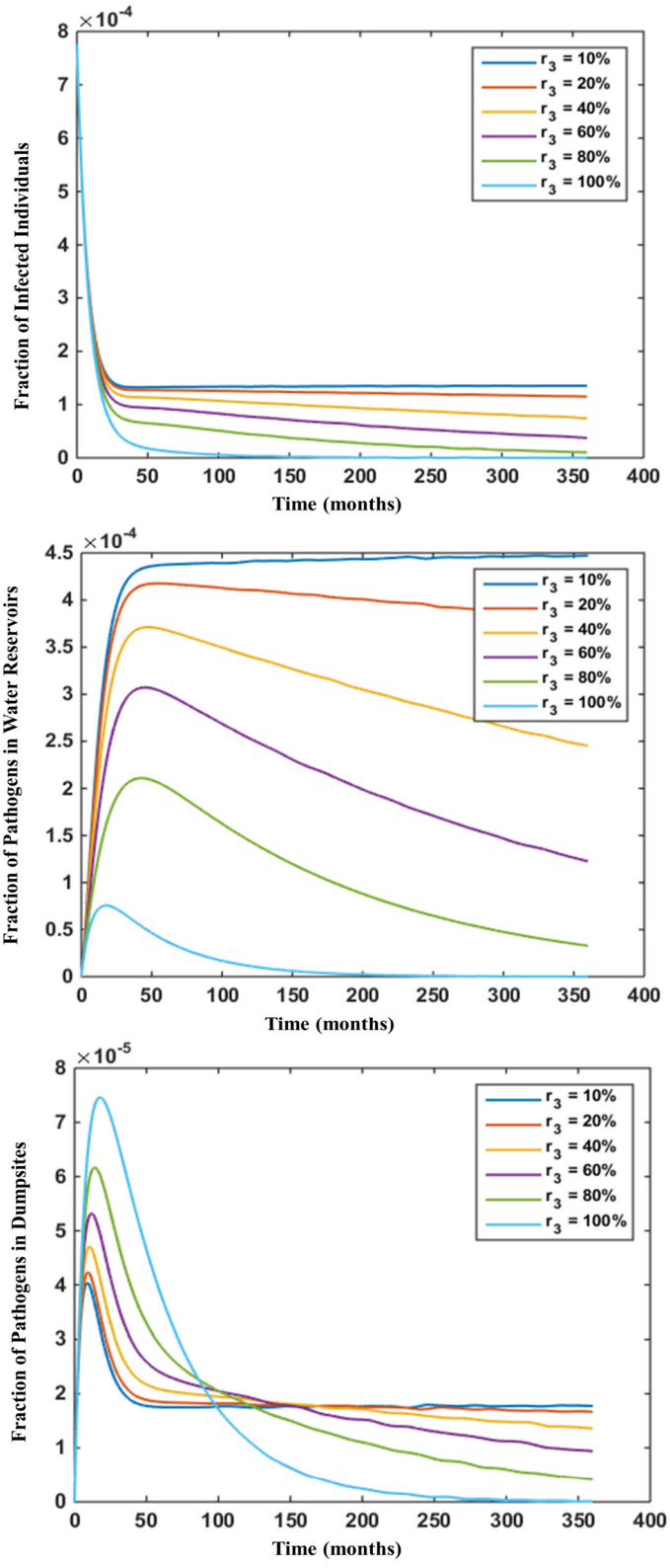

Figure 6 Dynamic behavior of the fraction of infected individuals (top), fraction of pathogens in water reservoirs (middle), and fraction of pathogens in dumpsites (bottom), with $r_1 = 65\%$, $r_2 = 35\%$, and varying r_3 from 10%, 20%, 40%, 60%, 80%, and 100%

directly affect the fraction of pathogens in dumpsites. Similarly, Figs. 5 and 6 show that at starting values of $r_2 = 35\%$ and $r_3 = 10\%$, respectively, the outbreak seems to maintain a steady state of the fraction of infected individuals, fraction of pathogens in water reservoirs, and fraction of pathogens in dumpsites.

Figure 7 displays the dynamic behavior of the fraction of infected individuals and the fraction of pathogens in water reservoirs and dumpsites with varying the coverage of two or three services at a time. Looking at the extreme case where $(r_1, r_2, r_3) = (80, 70, 50)$, the fraction of infected individuals (Fig. 7(top)) and the fraction of pathogens in water reservoirs (Fig. 7(middle)) are at the lowest. However, this does not reduce the fraction of pathogens in dumpsites (Fig. 7(bottom)) to be at the lowest. The cases of $(r_1, r_2, r_3) = (65, 70, 10)$ and $(80, 70, 10)$ have lower peaks than those of $(r_1, r_2, r_3) = (80, 70, 50)$. This shows that an increase in the coverage of MSW service (r_3) or an improvement in waste or garbage management does not reduce the fraction of pathogens in dumpsites within the first 150 months. The fraction of pathogens will eventually be reduced to zero, but over a long time. In other words, better MSW management means that garbage or the pathogens in the garbage are less likely to get into water reservoirs, and a disease is less likely to be transmitted to individuals via water. This improvement cuts the transmission pathway where pathogens in dumpsites can get into water, but not the fraction of pathogens in dumpsites.

Consequently, an increase in the coverage of WST service (r_2) has a greater impact (short-term) on the fraction of pathogens in dumpsites than an increase in the coverage of MSW service (r_3). WST has a direct impact on the fraction of pathogens in dumpsites. In many developing countries, wastewater and dumpsites are in direct contact with each other. Thus, wastewater treatment reduces the fraction of pathogens in dumpsites.

The results can be explained using Fig. 1. An increase in the coverage of DWS service (r_1) also affects the fraction of pathogens in dumpsites. Figure 1 shows that a change in r_1 affects the fraction of infected individuals, which affects the quantity of infected garbage/waste. Also, Fig. 1 shows that a change in the coverage of MSW service (r_3) has the least impact on the fraction of pathogens in dumpsites, as it does not affect compartment D directly. Better solid waste management means that pathogens in garbage are less likely to get into compartment W. This leads to fewer pathogens in water reservoirs, which yields a smaller fraction of infected individuals and less infected garbage.

Figure 7(bottom) also shows that the fraction of pathogens in dumpsites is at the lowest when $(r_1, r_2, r_3) = (80, 70, 10)$. This implies that an increase in the coverage of DWS service (r_1) and WST service (r_2) affects the fraction of pathogens in dumpsites. Overall, an increase in variable r_1 or r_2 alone has less impact on the fraction of infected individuals. With increased coverage of DWS and WST services, the 10% coverage of MSW service (r_3) is enough to improve the situation of a cholera outbreak in Haiti according to Fig. 7(bottom) for approximately the first 100 months. This is an important implication.

In Fig. 7(bottom), the cases of $(r_1, r_2, r_3) = (65, 70, 10)$ and $(80, 70, 10)$ result in the lowest peaks. This implies that a change in the coverage of WST service (r_2) may have the greatest impact on the fraction of pathogens in dumpsites. An increase in the coverage of DWS service (r_1) delineates these two lines (see 50 to 150 months). For $(r_1, r_2, r_3) = (65, 70, 50)$ and $(80, 70, 50)$ where $r_2 = 70$, the peaks are the second lowest. For $(r_1, r_2, r_3) = (65, 35, 10)$ and $(80, 35, 10)$, where $r_2 = 35$, the peaks occur approximately at the same position and at the highest. That is, it takes longer to reduce the fraction of pathogens in dumpsites

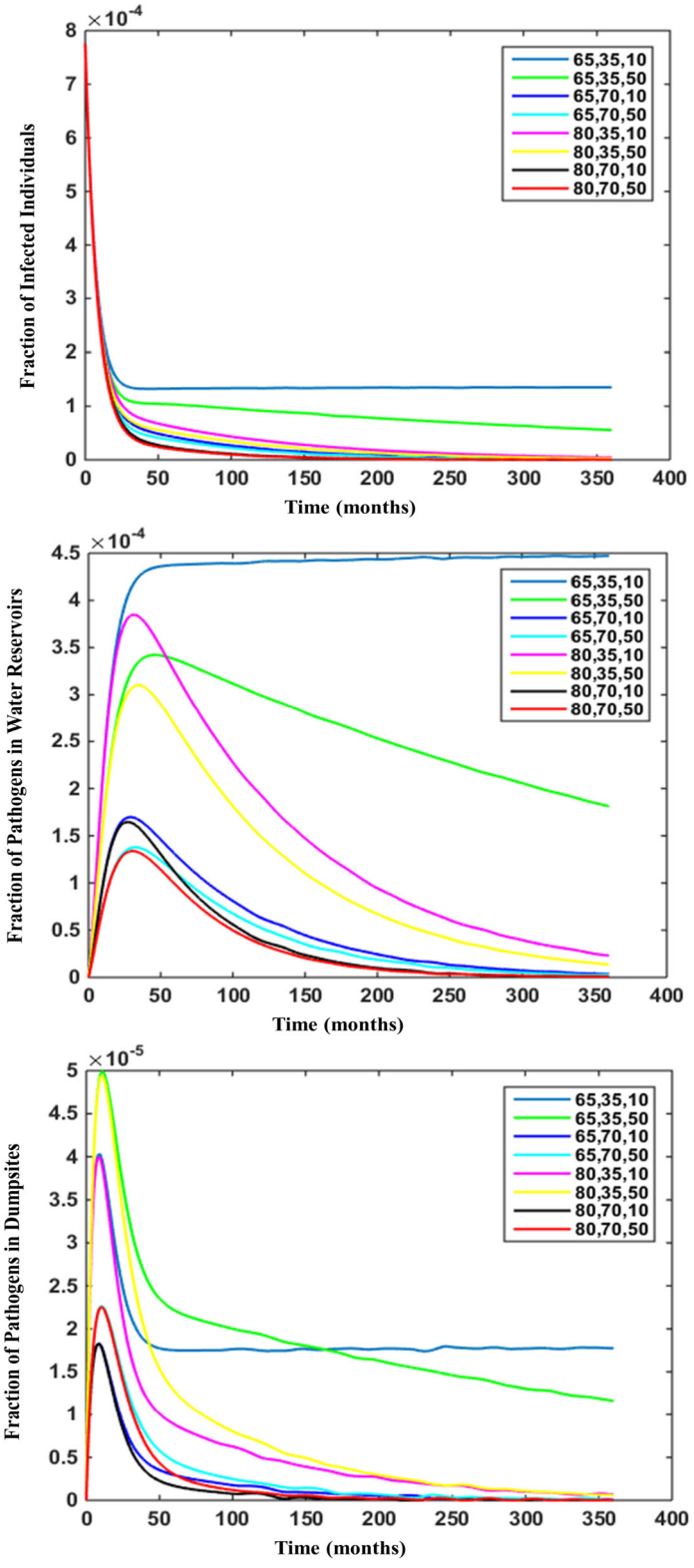

Figure 7 Effects of improving DWS, WST, and MSW services coverage (r_1, r_2, and r_3) on the fraction of infected individuals and the fraction of pathogens in water reservoirs and dumpsites that are predicted by model (3.2)

that have less improvement in DWS. In summary, the coverage of WST service (r_2) plays a significant role in reducing the fraction of pathogens in dumpsites. The same pattern happens for any of the two lines where r_2 and r_3 are the same with only a change in r_1. Peaks at any of the two lines occur at the same position. However, the decline in the fraction of pathogens (afterward) depends on the r_1 value.

Figure 7(bottom) illustrates that when r_1 and r_2 are the same, with only a change in r_1, there are intersections between any two selected observed lines. The coverage of MSW service (r_3) has a long-term impact. It reduces the fraction of pathogens significantly after approximately 170 months. In contrast, the coverage of DWS service (r_1) changes the fraction of pathogens significantly from about 25 to 100 months (the time after where the peak occurs). Consequently, decision makers must consider short-term and long-term goals depending on the budget at that time. The timing of eliminating a disease may be of concern.

Figure 8 confirms that there is a threshold value. When fixing the value of r_3, the coverage of DWS service (r_1) and the coverage of WST service (r_2) must be maintained. At the line where $(r_1, r_2, r_3) = (60, 30, 10)$, the fraction of infected individuals, the fraction of pathogens in water reservoirs, and the fraction of pathogens in dumpsites are out of control.

This study suggests that controlling and preventing waterborne diseases could be achieved by improving the service coverage of WST and MSW, to be sufficient, to protect water reservoirs and dumpsites from contamination. However, improving the service coverage of the DWS service could have the most impact among all of the WatSan services. Therefore, the WatSan service impact is explored as follows.

The results obtained in Table 5 are used as the projection of the fraction of the infected population for the next five years to cope with the 10-year plan which ends in 2022. The current data of coverage of WatSan services in 2017 from UNICEF [69] are used as the current situation (scenario 1). In scenario 1, the coverage of DWS, WST, and MSW services is 65%, 35%, and 10%, respectively. These percentages correspond to the values of $r_1 = 0.65$, $r_2 = 0.35$, and $r_3 = 0.10$, respectively. These values, with other parameter values given in Table 4, lead to $\mathcal{R}_0 = 1.0073$. In addition, the percentage reduction in the infected population is calculated by comparing the fraction of the infected population to the baseline, computed from the parameter values in Table 4. There is a 66.0674% reduction in the fraction of the infected population for scenario 1. By fixing all parameter values in scenario 1 except the coverage of each WatSan service, the threshold service coverage for each WatSan service that makes $\mathcal{R}_0 = 1$ is 65.28% of the service coverage of DWS (r_1), or 35.49% of the service coverage of WST (r_2), or 13.95% of the service coverage of MSW (r_3). A little improvement in each WatSan service while maintaining the other services would alleviate the disease outbreak. The experiments are extended by increasing or decreasing the percentage of r_1, r_2, and r_3 by 5% from scenario 1, as shown in Table 5. Scenarios 2–8 decrease r_1, r_2, and r_3, while scenarios 9–15 increase r_1, r_2, and r_3 by 5% from scenario 1. It is found that decreasing r_1, r_2, or r_3 from scenario 1 while maintaining the other services could result in a reduction in the infected population that is worse than scenario 1. $\mathcal{R}_0$ in scenarios 2–8 are higher than $\mathcal{R}_0$ in scenario 1. In scenarios 9–15, increasing r_1, r_2, or r_3 from scenario 1 while maintaining the other services could result in a percentage reduction in the infected population that is better than scenario 1. In addition, $\mathcal{R}_0$ in scenarios 9–15 is less than $\mathcal{R}_0$ in scenario 1. The impact of decreasing r_1, r_2, or r_3 is greater

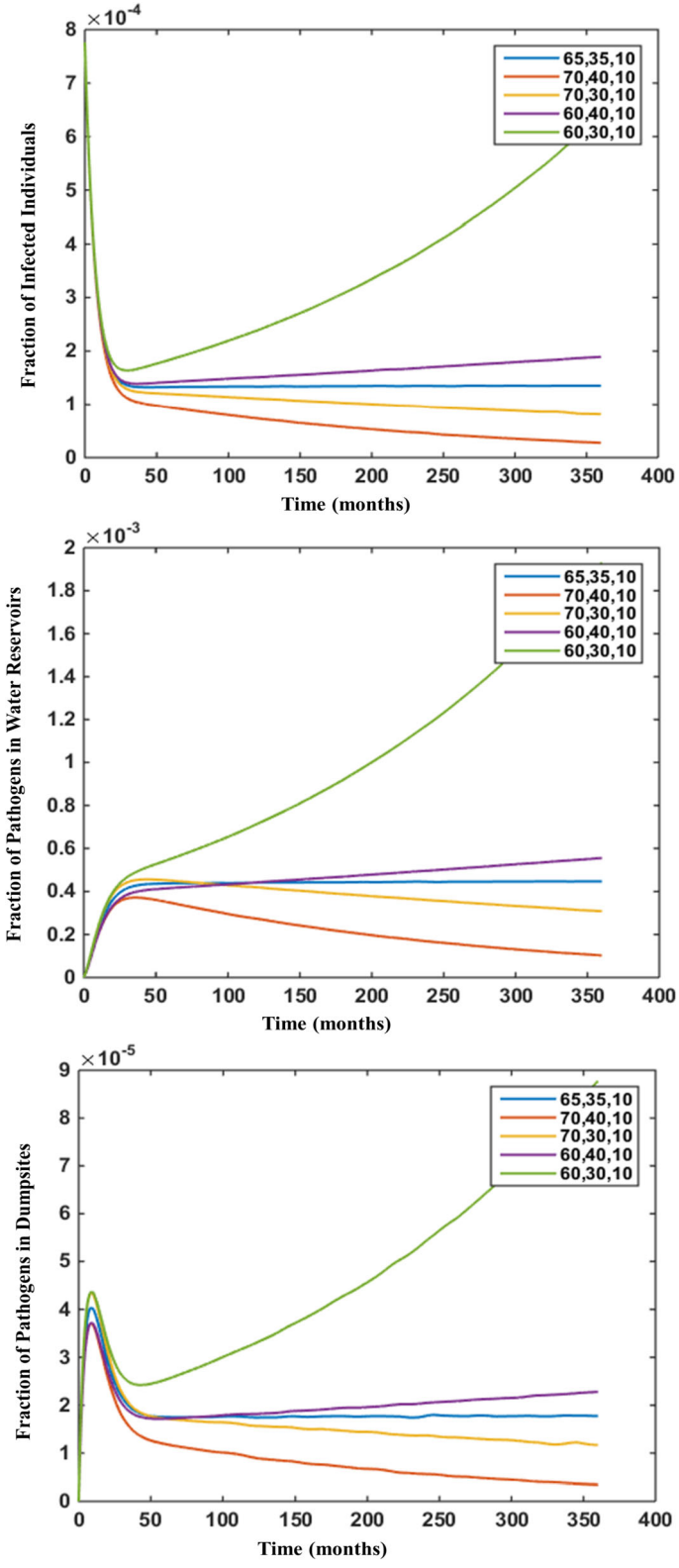

Figure 8 Effects of improving DWS and WST services coverage (r_1 and r_2) on the fraction of infected individuals and the fraction of pathogens in water reservoirs and dumpsites that are predicted by model (3.2)

Table 5 Impact of WatSan services on the percentage reduction in the infected population

Scenarios	r_1	r_2	r_3	% reduction of infected population	$\mathcal{R}_0$
1	0.6500	0.3500	0.1000	66.0674	1.0073
2	0.6000	0.3500	0.1000	36.0778	1.1370
3	0.6500	0.3000	0.1000	48.4736	1.0820
4	0.6500	0.3500	0.0500	60.0196	1.0158
5	0.6000	0.3000	0.1000	8.5914	1.2217
6	0.6000	0.3500	0.0500	32.9038	1.1466
7	0.6500	0.3000	0.0500	46.1522	1.0912
8	0.6000	0.3000	0.0500	3.3407	1.2321
9	0.7000	0.3500	0.1000	75.5579	0.8776
10	0.6500	0.4000	0.1000	70.6619	0.9325
11	0.6500	0.3500	0.1500	63.0107	0.9980
12	0.7000	0.4000	0.1000	80.0980	0.8128
13	0.7000	0.3500	0.1500	76.2678	0.8695
14	0.6500	0.4000	0.1500	71.6331	0.9239
15	0.7000	0.4000	0.1500	80.5796	0.8053

than the impact of increasing r_1, r_2, or r_3 when comparing the percentage reduction in the infected population for scenarios 2–8 and 9–15. The result in scenario 5 shows that decreasing r_1 and r_2 decreases the reduction in the infected population significantly. Scenario 12 demonstrates that increasing r_1 and r_2 increases the reduction in the infected population remarkably. However, the impact on the reduction in the fraction of the infected population is greater for scenario 5 (from 66.0674 % to 8.5914%) than for scenario 12 (from 66.0674 % to 80.0980%).

Thus, it is concluded that maintaining the service coverage of r_1 and r_2 is important to prevent the transmission of waterborne diseases. Figure 8 shows the impact of improving and reducing r_1 and r_2. Reducing both services could make water reservoirs and dumpsites more contaminated. This impacts the fraction of the infected population. Our study shows that maintaining the service coverage of MSW (r_3) while improving the service coverage of DWS and WST (r_1 and r_2) could have the most health impact on a community. Thus, our study suggests that shifting the budget away from improving the service coverage of MSW to just maintaining this service is a desirable policy. In addition, the shifted budget could be used for improving the service coverage of DWS and WST instead. According to the 2013–2022 plan to combat cholera in Haiti, the budget allocation for improving the service coverage of DWS, WST, and MSW is 49.5%, 28.1%, and 22.4%, respectively. This allocation is suitable for fighting cholera. However, to efficiently eliminate cholera from Haiti, our study recommends that the allocated budget of 22.4% to improve MSW should be reduced. This reduction in the budget should be used to improve the service coverage of DWS and WST by emphasizing the improvement of DWS.

As described earlier, proposed model (2.1) is suitable when there are other pathogen reservoirs that are important in the disease transmission process. This study extends the Tien and Earn (2010) model that takes into account only one pathogen reservoir, i.e., a water reservoir [28]. This study finds that environmental factors play an important role in controlling and preventing disease outbreaks. Considering the water compartment (W) and dumpsite compartment (D) is more effective than considering only compartment W if dumpsites in a particular community are contaminated. Additionally, our mathematical model quantifies the qualitative data that many researchers [41] have agreed upon. Wat-

San services do indeed prevent and control waterborne diseases. According to this paper, WatSan services should not be given equal priority.

5 Conclusions

This paper presents the modified *SIR* model by incorporating access to WatSan services and the prevalence of open dumpsites as pathogen enablers. The proposed model is rigorously analyzed to gain insights into its dynamic behavior. Then, it is used to investigate the health impact of WatSan service deficits on waterborne disease transmission. Using cholera as our case study, our analysis yielded some useful new insights into the dynamics and control of waterborne diseases. The basic reproductive number ($\mathcal{R}_0$) of the model is derived and given in Equation (3.6) by using the next generation method. It was found that the disease-free equilibrium is globally asymptotically stable whenever $\mathcal{R}_0 \leq 1$ as guaranteed by Theorem 3.2. When $\mathcal{R}_0 > 1$, the endemic equilibrium (EE) of the proposed model exists and is globally asymptotically stable, which is consistent with Theorem 3.4. These theoretical studies reveal that the disease dies out when $\mathcal{R}_0 \leq 1$ and the disease becomes endemic when $\mathcal{R}_0 > 1$. Therefore, control strategies that set $\mathcal{R}_0 \leq 1$ would generate public health benefits in making strategy decisions after infectious diseases appear. The appropriate parameter values of the model were obtained by comparing the predicted data with real data from the 2010 cholera outbreak in Haiti. These parameter values were used to investigate the most sensitive model parameters in controlling and preventing cholera outbreaks. It was found that β_W is the most sensitive parameter to the initial transmission, and r_1 is the most sensitive parameter to the initial decrease in disease transmission. The coverage of DWS services is the most sensitive parameter to the initial decrease in disease transmission in relation to the coverage of WST and MSW services. In other words, this study verifies that improving the coverage of DWS services is the most effective intervention to control a cholera outbreak. Analyzing the contour plots of surface $\mathcal{R}_0$ as a function of the service coverages (r_1, r_2, and r_3) demonstrates that improving all the service coverages (DWS, WST, and MSW) would certainly decrease the initial disease transmission. Moreover, analyses of single and double control strategies showed that control strategies that involve the combined improvement of multiple water and sanitation services are better at controlling the initial disease transmission and reducing the overall infections than single strategies.

Therefore, this study suggests that to control the spread of infectious waterborne diseases like cholera, the first priority should be to improve the access to safe drinking water supplies. As funding and other resources permit, the effectiveness of control measures would subsequently be increased by adding improved treatment of contaminated water sources and improved management of open dumpsites to the improved drinking water supply. To some degree these results are intuitive. Certainly, to improve access to safe drinking water supplies, the treatment of contaminated water sources would be required. By similar reasoning, improved management of open dumpsites could reduce the extent of leachate contamination of groundwater and control harmful runoff into surface water bodies that serve as sources for drinking water supplies. Thus, prioritizing the access to safe drinking water supplies is likely to require improved treatment of contaminated water bodies and improved management of community dumpsites as effective strategies for cutting the transmission pathways of waterborne diseases like cholera. This is an important implication and a contribution of this study.

The comparative results of the effects of each service are illustrated in Table 5 for the case of enteric diarrheal disease (EDD). In this case, we found that improving DWS and WST services yields a higher reduction in EDD than improvements in the MSW service. This result suggests that WatSan service managers should prioritize investment in DWS and WST services over the MSW service in a strategy to control the incidence of EDD from waterborne sources. The budget for infrastructure services may be limited, as it is in many low- and middle-income countries. Therefore, this strategy could be useful in budget allocation for improving WatSan services to manage outbreaks of waterborne diseases. Furthermore, model (2.1) is formulated by incorporating the state variables of WatSan services and the incidence of EDD. Thus, if reliable data on the parameters of a particular disease and the unit costs of WatSan services are available, model (2.1) can be applied to design optimization algorithms for budget allocation in improving WatSan services, to minimize the size of the infected population during disease outbreaks. This is the focus of our future work.

Acknowledgements
The authors would like to express their gratitude to the anonymous referee for helpful suggestions and comments which led to improvements in our original manuscript.

Funding
This research is supported by the Institute for the Promotion of Teaching Science and Technology (IPST), Thailand, under the Research Fund for DPST (Development and Promotion of Science and Technology Talents Project) Graduate with First Placement (Grant no. 033/2559).

Availability of data and materials
The authors declare that all data and material in the paper are available and veritable.

Competing interests
The authors declare that they have no competing interests.

Authors' contributions
RC and GEL conceived this research. RC developed the SIWDR model, conducted the numerical simulations, performed analysis and drafted the manuscript. GEL revised the manuscript. WC participated in the interpretation of the data, and revised the manuscript. All authors read and approved the final manuscript.

Author details
[1]School of Management Technology, Sirindhorn International Institute of Technology, Thammasat University, Pathum Thani, Thailand. [2]Department of Engineering Systems and Environment, University of Virginia, Charlottesville, Virginia, USA. [3]Department of Mathematics, Faculty of Science, King Mongkut's University of Technology Thonburi, Bangkok, Thailand.

Publisher's Note

Received: 5 March 2021 Accepted: 17 August 2021 Published online: 06 September 2021

References

1. Griffiths, J.K.: Waterborne diseases. In: International Encyclopedia of Public Health, 2nd edn., pp. 388–401. Elsevier, Amsterdam (2017)
2. Sharma, S., Kumari, N.: Dynamics of a waterborne pathogen model under the influence of environmental pollution. Appl. Math. Comput. **346**, 219–243 (2019)
3. World Health Organization: Drinking-water (2020). https://www.who.int/news-room/fact-sheets/detail/drinking-water. Accessed 23 May 2021
4. World Health Organization (WHO, and UNICEF): Global water supply and sanitation assessment 2000 report (2000). http://www.who.int/water_sanitation_health/monitoring/jmp2000.pdf. Accessed 23 May 2021
5. Centers for Disease Control and Prevention: Cholera in Haiti (2014). https://www.cdc.gov/cholera/haiti/index.html. Accessed 23 May 2021
6. United Nations: Yemen: as cholera surges again, UN and partners double down on vaccination efforts (2018). https://news.un.org/en/story/2018/10/1022062. Accessed 23 May 2021
7. Fewtrell, L., Kaufmann, R.B., Kay, D., Enanoria, W., Haller, L., Colford, J.M. Jr.: Water, sanitation, and hygiene interventions to reduce diarrhoea in less developed countries: a systematic review and meta-analysis. Lancet Infect. Dis. **5**(1), 42–52 (2005)

8. Waddington, H., Snilstveit, B.: Effectiveness and sustainability of water, sanitation, and hygiene interventions in combating diarrhoea. J. Dev. Eff. **1**(3), 295–335 (2009)
9. Puri, A., Kumar, M., Johal, E.: Solid-waste management in Jalandhar city and its impact on community health. Indian J. Occup. Environ. Med. **12**(2), 76–81 (2008)
10. Cruvinel, V.R.N., Zolnikov, T.R., Bashash, M., Marques, C.P., Scott, J.A.: Waterborne diseases in waste pickers of Estrutural, Brazil, the second largest open-air dumpsite in world. Waste Manag. **99**, 71–78 (2019)
11. Kjeldsen, P.: Groundwater pollution source characterization of an old landfill. J. Hydrol. **142**(1–4), 349–371 (1993)
12. Gerba, C.P.: Microbial pathogens in municipal solid waste. In: Palmisano, A.C., Barlaz, M.A. (eds.) Microbiology of Solid Waste, pp. 155–173. CRC Press, New York (1996)
13. Giusti, L.: A review of waste management practices and their impact on human health. Waste Manag. **29**(8), 2227–2239 (2009)
14. Al-Gheethi, A., Noman, E., Jeremiah David, B., Mohamed, R., Abdullah, A., Nagapan, S., Hashim Mohd, A., et al.: A review of potential factors contributing to epidemic cholera in Yemen. J. Water Health **16**(5), 667–680 (2018)
15. Prüss, A., Kay, D., Fewtrell, L., Bartram, J.: Estimating the burden of disease from water, sanitation, and hygiene at a global level. Environ. Health Perspect. **110**(5), 537–542 (2002)
16. Esrey, S.A., Feachem, R.G., Hughes, J.M.: Interventions for the control of diarrhoeal diseases among young children: improving water supplies and excreta disposal facilities. Bull. World Health Organ. **63**(4), 757–772 (1985)
17. Mara, D., Lane, J., Scott, B., Trouba, D.: Sanitation and health. PLoS Med. **7**(11), e1000363 (2010)
18. World Health Organization: Diarrhoeal disease (2017). https://www.who.int/news-room/fact-sheets/detail/diarrhoeal-disease. Accessed 23 May 2021
19. Prüss-Üstün, A., Wolf, J., Corvalán, C., Bos, R., Neira, M.: Preventing disease through healthy environments: a global assessment of the burden of disease from environmental risks. World Health Organization (2016)
20. Prüss, A., Havelaar, A.: The global burden of disease study and applications in water, sanitation and hygiene. Water Qual. Guidel. Stand. Health **1**(1), 43–60 (2001)
21. Clasen, T., Schmidt, W., Rabie, T., Roberts, I., Cairncross, S.: Interventions to improve water quality for preventing diarrhoea: systematic review and meta-analysis. BMJ **334**(7597), 782 (2010)
22. Haller, L., Hutton, G., Bartram, J.: Estimating the costs and health benefits of water and sanitation improvements at global level. J. Water Health **5**(4), 467–480 (2007)
23. Clasen, T., Alexander, K., Sinclair, D., Boisson, S., Peletz, R., Chang, H., Majorin, F., Cairncross, S.: Interventions to improve water quality for preventing diarrhoea. Cochrane Database Syst. Rev. **10** (2015)
24. Lanata, C.F., Huttly, S.R., Yeager, B.A.: Diarrhea: whose feces matter? Reflections from studies in a Peruvian shanty town. Pediatr. Infect. Dis. J. **17**(1), 7–9 (1998)
25. Genser, B., Strina, A., Teles, C.A., Prado, M.S., Barreto, M.L.: Risk factors for childhood diarrhea incidence: dynamic analysis of a longitudinal study. Epidemiology **17**(6), 658–667 (2006)
26. Barreto, M.L., Genser, B., Strina, A., Assis, A.M.O., Rego, R.F., Teles, C.A., Prado, M.S., Matos, S.M., Santos, D.N., dos Santos, L.A., et al.: Effect of city-wide sanitation programme on reduction in rate of childhood diarrhoea in northeast Brazil: assessment by two cohort studies. Lancet **370**(9599), 1622–1628 (2007)
27. Norman, G., Pedley, S., Takkouche, B.: Effects of sewerage on diarrhoea and enteric infections: a systematic review and meta-analysis. Lancet Infect. Dis. **10**(8), 536–544 (2010)
28. Tien, J.H., Earn, D.J.: Multiple transmission pathways and disease dynamics in a waterborne pathogen model. Bull. Math. Biol. **72**(6), 1506–1533 (2010)
29. Eisenberg, M.C., Robertson, S.L., Tien, J.H.: Identifiability and estimation of multiple transmission pathways in cholera and waterborne disease. J. Theor. Biol. **324**, 84–102 (2013)
30. Robertson, S.L., Eisenberg, M.C., Tien, J.H.: Heterogeneity in multiple transmission pathways: modelling the spread of cholera and other waterborne disease in networks with a common water source. J. Biol. Dyn. **7**(1), 254–275 (2013)
31. Bertuzzo, E., Casagrandi, R., Gatto, M., Rodriguez-Iturbe, I., Rinaldo, A.: On spatially explicit models of cholera epidemics. J. R. Soc. Interface **7**(43), 321–333 (2010)
32. Mari, L., Bertuzzo, E., Righetto, L., Casagrandi, R., Gatto, M., Rodriguez-Iturbe, I., Rinaldo, A.: Modelling cholera epidemics: the role of waterways, human mobility and sanitation. J. R. Soc. Interface **9**(67), 376–388 (2012)
33. Gatto, M., Mari, L., Bertuzzo, E., Casagrandi, R., Righetto, L., Rodriguez-Iturbe, I., Rinaldo, A.: Generalized reproduction numbers and the prediction of patterns in waterborne disease. Proc. Natl. Acad. Sci. USA **109**(48), 19703–19708 (2012)
34. Wang, Y., Cao, J.: Global dynamics of a network epidemic model for waterborne diseases spread. Appl. Math. Comput. **237**, 474–488 (2014)
35. Collins, O.C., Govinder, K.S.: Incorporating heterogeneity into the transmission dynamics of a waterborne disease model. J. Theor. Biol. **356**, 133–143 (2014)
36. Tuite, A.R., Tien, J., Eisenberg, M., Earn, D.J., Ma, J., Fisman, D.N.: Cholera epidemic in Haiti, 2010: using a transmission model to explain spatial spread of disease and identify optimal control interventions. Ann. Intern. Med. **154**(9), 593–601 (2011)
37. Collins, O.C., Robertson, S.L., Govinder, K.S.: Analysis of a waterborne disease model with socioeconomic classes. Math. Biosci. **269**, 86–93 (2015)
38. Mari, L., Casagrandi, R., Bertuzzo, E., Rinaldo, A., Gatto, M.: Conditions for transient epidemics of waterborne disease in spatially explicit systems. R. Soc. Open Sci. **6**, 181517 (2019)
39. Mwasa, A., Tchuenche, J.M.: Mathematical analysis of a cholera model with public health interventions. Biosystems **105**, 190–200 (2011)
40. Wanga, Y., Cao, J.: Global stability of a multiple infected compartments model for waterborne diseases. Commun. Nonlinear Sci. Numer. Simul. **19**, 3753–3765 (2014)
41. Keusch, G.T., Fontaine, O., Bhargava, A., BoschiPinto, C., Bhutta, Z.A., Gotuzzo, E., Laxminarayan, R.: Diarrheal diseases. In: Jamison, J.T., Breman, J.G., Measham, A.R. (eds.) Disease Control Priorities in Developing Countries, 2nd edn., pp. 371–388. Oxford University Press, New York (2006)
42. Hethcote, H.M.: The mathematics of infectious diseases. SIAM Rev. **42**, 599–963 (2000)
43. Van den Driessche, P., Watmough, J.: Further notes on the basic reproduction number. In: Brauer, F., van den Driessche, P., Wu, J. (eds.) Mathematical Epidemiology, pp. 159–178. Springer, Berlin (2008)

44. Hale, J.K.: Ordinary Differential Equations. Wiley, New York (1969)
45. Carr, J.: Applications of Centre Manifold Theory. Springer, New York (2012)
46. Castillo-Chavez, C., Song, B.: Dynamical models of tuberculosis and their applications. Math. Biosci. Eng. **1**(2), 361–404 (2004)
47. Zhou, T.: Global stability. In: Dubitzky, W., Wolkenhauer, O., Cho, K.H., Yokota, H. (eds.) Encyclopedia of Systems Biology, p. 842. Springer, New York (2013)
48. Korobeinikov, A., Wake, G.C.: Lyapunov functions and global stability for SIR, SIRS, and SIS epidemiological models. Appl. Math. Lett. **15**(8), 955–960 (2002)
49. Vargas-De-León, C.: On the global stability of SIS, SIR and SIRS epidemic models with standard incidence. Chaos Solitons Fractals **44**(12), 1106–1110 (2011)
50. Roop-O, P., Chinviriyasit, W., Chinviriyasit, S.: The effect of incidence function in backward bifurcation for malaria model with temporary immunity. Math. Biosci. **265**, 47–64 (2015)
51. Nudee, K., Chinviriyasit, S., Chinviriyasit, W.: The effect of backward bifurcation in controlling measles transmission by vaccination. Chaos Solitons Fractals **123**, 400–412 (2019)
52. LaSalle, J.P.: The Stability of Dynamical Systems. Hamilton Press, New Jersey (1976)
53. Centers for Disease Control and Prevention: Eliminating cholera transmission from Haiti (2018). https://www.cdc.gov/globalhealth/countries/haiti/what/eliminating-cholera-haiti.html. Accessed 23 May 2021
54. World Bank: Population in largest city (2020). https://data.worldbank.org/indicator/EN.URB.LCTY. Accessed 23 May 2021
55. The World Bank: Birth rate, crude (per 1,000 people)—Haiti (2019). https://data.worldbank.org/indicator/SP.DYN.CBRT.IN?locations=HT. Accessed 23 May 2021
56. The World Bank: Death rate, crude (per 1,000 people)—Haiti (2019). https://data.worldbank.org/indicator/SP.DYN.CDRT.IN?locations=HT. Accessed 23 May 2021
57. Fung, I.C.H.: Cholera transmission dynamic models for public health practitioners. Emerg. Themes Epidemiol. **11**(1), 1 (2014)
58. King, A.A., Ionides, E.L., Pascual, M., Bouma, M.J.: Inapparent infections and cholera dynamics. Nature **454**(7206), 877–880 (2008)
59. World Health Organization: Cholera (2012). http://www.unicef.org/cholera/Chapter_1_intro/01_WHO_Cholera_Fact_sheet_107_July_2012.pdf. Accessed 23 May 2021
60. Hendrix, T.R.: The pathophysiology of cholera. Bull. N.Y. Acad. Med. **47**(10), 1169–1180 (1971)
61. UNICEF: Cholera toolkit (2013). http://www.unicef.org/cholera/Cholera-Toolkit-2013.pdf. Accessed 23 May 2021
62. World Health Organization: Progress on drinking-water and sanitation—2012 Update (2012). http://www.unicef.org/media/files/JMPreport2012.pdf. Accessed 23 May 2021
63. World Health Organization: 25 Years progress on sanitation and drinking water (2015). http://apps.who.int/iris/bitstream/handle/10665/177752/9789241509145_eng.pdf. Accessed 23 May 2021
64. Bras, A., Berdier, C., Emmanuel, E., Zimmerman, M.: Problems and current practices of solid waste management in Port-au-Prince (Haiti). Waste Manag. **29**(11), 2907–2909 (2009)
65. Pan American Health Organization: Atlas of cholera outbreak in La Hispaniola 2010–2016 (2016). https://www3.paho.org/hq/images/Atlas_IHR/CholeraHispaniola/atlas.html. Accessed 23 May 2021
66. Mukandavire, Z., Smith, D.L., Morris, J.G. Jr.: Cholera in Haiti: reproductive numbers and vaccination coverage estimates. Sci. Rep. **3**, 997 (2013)
67. Chitnis, N., Hyman, J.M., Cushing, J.M.: Determining important parameters in the spread of malaria through the sensitivity analysis of a mathematical model. Bull. Math. Biol. **70**(5), 1272–1296 (2008)
68. Ministry of Public Health and Population National Directorate for Water Supply and Sanitation, Republic of Haiti: National plan for the elimination of cholera in Haiti 2013–2022 (2013). https://www.paho.org/hq/dmdocuments/2013/cholera-haiti-nat-plan-elim-2013-2022.pdf. Accessed 23 May 2021
69. UNICEF: Progress on household drinking water, sanitation and hygiene, 2000–2017 (2019). https://data.unicef.org/resources/progress-drinking-water-sanitation-hygiene-2019/#. Accessed 23 May 2021